ChemComm

Accepted Manuscript

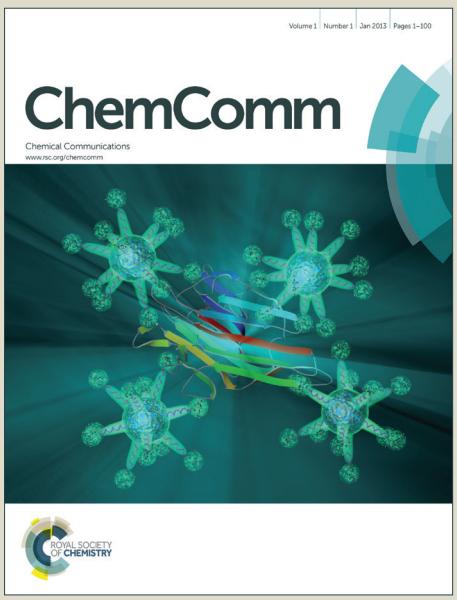

ROYAL SOCIETY OF CHEMISTRY

www.rsc.org/chemcomm

ChemComm

RSCPublishing

COMMUNICATION

Enhancement of Cancer Specific Delivery Using Ultrasound Active Bio-originated Particles

Cite this: DOI: 10.1039/x0xx00000x

DOI: 10.1039/x0xx00000x

www.rsc.org/

Young Il Yoon,[a,g] Kook Yun Ju,[b,g] Hee-Sang Cho,[c] Kyeong Nam Yu,[d] Jae Jun Lee,[e] Gook Jun Ahn,[e] Soo-Hong Lee,[f] Myung Haing Cho,[d] Hak Jong Lee*,[a] Jin-Kyu Lee*,[b] Tae-Jong Yoon*[c]

A hybrid multifunctional particle comprising of microbbule (MB), liposome (Lipo), and Fe ion chelated melanin nanoparticle (MNP(Fe)) was applied for ultrasound mediated cancer targeting as a theranostics agent.

One of the major advantages of theranostic materials is their ability to simultaneously perform multiple functions. A single particle can be used to diagnose a disease and to image cells.[1-3] To date, most of the organic, inorganic, and compound theranostic agents developed contain polymer particles, magnetic nanoparticles, quantum dots, and novel metal substrates. While these theranostic agents exhibit multiple attractive properties, namely an enhanced bio-availability with prolonged circulation time, preferential tumor accumulation owing to the enhanced permeability and retention (EPR) effect and imaging compatibility with existing detection modalities (e.g., magnetic resonance imaging or optical excitation), their clinical translation remains challenging. [4-7] The potential toxicity of the constituent materials (especially the inorganic nanoparticles) raises significant safety concerns and toxicological evidence, all of which need to be carefully addressed prior to their clinical applications.[8-10]

Microbubbles (micro-meter sized bubble, MBs) and liposomes (Lipos) are emerging biocompatible materials for cancer diagnosis and treatment, and therefore represent a safer alternative to conventional theranostic agents.[11, 12] By coupling MBs and Lipos as a complex, this concept material has been shown to achieve simultaneous ultrasound (US) imaging of cells as well as highly efficient targeted delivery of therapeutic loads.[13, 14] Moreover, when integrated with super-paramagnetic iron-oxide nanoparticles, the assembly provided dual contrast in both magnetic resonance (MR) and US imaging.[15] While such formulation enabled multi-model imaging, the incorporation of inorganic particles reduces its biocompatibility and limits its clinical potential, as with conventional theranostic agents.

Herein, we report the preparation of a fully biocompatible and multifunctional hybrid complex comprising of MB, Lipo and Fe^{3+} ion-chelated melanin nanoparticles (MNPs) that can enable dual US-MR imaging as well as enhanced gene delivery. Leveraging on the high Fe^{3+} loading capacity of MNPs, the resultant complex achieves MR contrast from only biocompatible chemicals.[16] The resulting complex particles generated high contrast under normal US illumination, as MBs oscillated and generated acoustic waves. For the delivery of therapeutic material, we burst MBs in situ by applying higher acoustical pressure (US flash); this unloaded Lipos and MNPs from MBs as well as temporarily permeabilized cellular membrane for efficient delivery.[17, 18] We further functionalized the complex particles with antibody and showed 1) specific targeting to tumor cells and 2) US-stimulated effective delivery of the linked MNPs and Lipos into the cells. After localized application of moderate high acoustic pressure, we observed enhancements in both the MRI signal as well as the therapeutic effect by the internalized MNP and Lipo particles.

After homogenous mixing of the various phospholipids and cholesterol, the MBs were synthesized by film formation and by the bubbling of hydrophobic SF_6 gas (8 μL/mL), which was accompanied by mechanical vibration. Similarly, the Lipos were produced *via* film formation, sonication, and extrusion (without gas). The shape and size distribution of the MBs and Lipos were characterized by microscopy, cryo-electron microscopy and dynamic light scattering (Fig. 1a and ESI Fig. S1). The synthesized MBs and Lipos were spherical, with an average diameter of 1.3 μm and 200 nm,

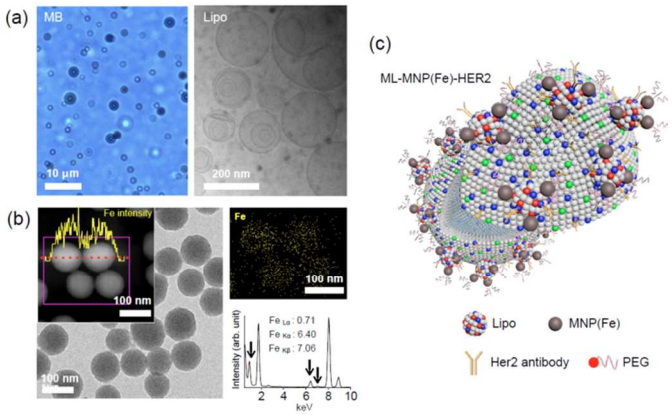

Fig. 1. Characterization of MB, Lipo and MNP(Fe) particles; The spherical shape of the MB and Lipo particles were confirmed with a microscope (a, left) and a cryo-electron microscope (a, right). Fe^{3+} ion chelated MNP, MNP(Fe) showed a spherical shape, as evident from the TEM analysis (b) and the intensity of the iron metal bound to the MNP surface (b, inset) was mapped by scanning-TEM (b, right-up). The qualification analysis was also conducted with TEM equipped with EDX, and several energy-dispersed peaks indicated the presence of iron metal (b, right-bottom, relevant peaks are marked with black arrows). The MB, Lipo and MNP(Fe) complexed particle was portrayed the schematic diagram (c)

respectively. The MB and Lipo cores comprise of a hydrophobic gas phase and a hydrophilic aqueous phase, respectively. During the preparation, we also added a hydrophobic dye (fluorescein isothiocyanate, G) for localizing the alkyl chain of the MB shell, and a red hydrophilic dye (Texas Red, R) for incorporation into the aqueous Lipo core (ESI Fig. S1).

The MNPs were produced with a modified protocol of previous methods (see ESI for details). Briefly, 780 µL of NaOH solution (1 M) was added into 90 mL of dopamine hydrochloride solution (2 mg/mL) under vigorous stirring at 50 °C to facilitate spontaneous oxidation of dopamine and polymerization to form MNPs. After 6 h, the particles were collected by centrifugation at 20,000 rpm (10 min) and washed several times with distilled water. The resulting spherical MNP particles had an average diameter of 100 nm and a regular size distribution. To incorporate magnetic property, 1 mg of MNPs was dissolved in a 2-mL Fe $(NO_3)_3 \cdot 6H_2O$ (1.85 mM) solution to chelate Fe^{3+} ions onto the *o*-dihydroxyl group of the catechol unit on the MNP surface. This process loaded 3 µmol of Fe^{3+} ions per mg MNP, as determined by an inductively coupled plasma-atomic emission spectroscopy. The chelation of Fe^{3+} ions was strongly maintained to the MNP surface at various pH levels (ESI Fig.

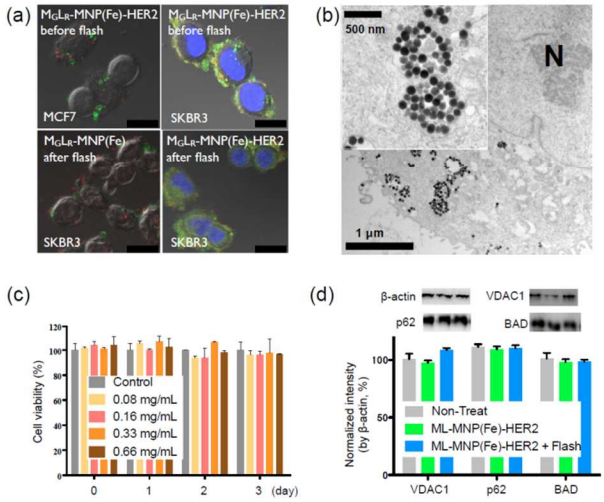

Fig. 2. Specific targeting, US flash effect, and assessment of cytotoxicity; (a, scale bar = 25 µm) Green and red fluorescent M_GL_R-MNP(Fe)-HER2 particles specifically recognized the Her2 receptor expressed in breast cancer cells (SKBR3) comparing with negative cells (MCF7, a, top-left). The HER2 conjugated particles were represented on the cell membranes (a, top-right, the blue color indicates the DAPI-stained nucleus). The non-antibody conjugated particles treated SKBR3 cells were rarely show fluorescence (a, bottom-left) after exposure to a US flash (MI = 0.61). But the M_GL_R-MNP(Fe)-HER2 particle treated SKBR3 cells with US flash exhibited the fluorescent dyes into the cell cytosol (a, bottom-right). The released MNP(Fe)s were found to localize within the cytoplasm of SKBR3 cells using bio-TEM analysis (b) and there was no change in the size and shape of the MNP (b, inset). ML-MNP(Fe)-HER2 and US flash treated-cells showed a viability > 90 % for various concentrations and culture times (c). For the cell cyto-toxicity assay that measured the protein levels, 0.66 mg/mL of the particles were added to the cells, which were then analyzed for the alteration of protein levels related to cell-organelle functions, using western blotting (d). These cells showed similar expression levels as the non-treated control cell. (All experiments in c and d were performed in triplicate. Data shows mean +/- SD)

S2). The Fe^{3+}-doped particle, MNP(Fe), was analyzed by scanning-transmission electron microscopy (STEM) (Fig. 1b). The loaded Fe^{3+} ions were homogeneously revealed onto the particle surface and were qualitatively analyzed using an STEM-equipped energy-dispersive x-ray spectrometer (EDX). The Fe^{3+} ion can thus efficiently cause the longitudinal (T_1) decrease of water protons as a T_1-weighted (T_1-*w*) MR contrast agent.

To prepare a hybrid of MB and Lipo (abbreviated to ML, Fig. S1a), 1,2-distearoyl-sn-glycero-3-phosphoethanolamine-N-[PDP(polyethylene glycol)-2000] (DSPE-PEG-SPDP) in MB was cross-linked with the sulfhydryl chemical functional group (-SH) after treating Traut's reagent with 1,2-dipalmitoyl-sn-glycero-3-phosphoethanolamine (DPPE) in Lipo (see ESI). The Ellman's reagent was used to determine the number of sulfhydryl groups present on the Lipos. The linking was characterized by detecting pyridine-2-thione (a leaving group) using UV-Vis spectroscopy. The average diameter of the ML was approximately 1.6 µm. Subsequently, the synthesized MNP(Fe) was attached onto the excess sulfhydryl moiety present on the Lipo of the ML complex, *via* a Schiff's base or a Michael addition reaction.[19] The ML-MNP(Fe) complex particles were treated with methoxy-poly(ethylene glycol) (PEG-SH, 2 kDa) to increase their solubility in aqueous buffers. For specific cancer cell targeting by the ML-MNP(Fe) particles, an antibody against human epidermal growth factor receptor 2 (HER2) was introduced to the particles by a typical half-antibody conjugation procedure, and the anchored antibodies were quantitatively analyzed by a protein determination method (see ESI, 70 nM HER2 antibody per mM DPPC of the particle).[20, 21]

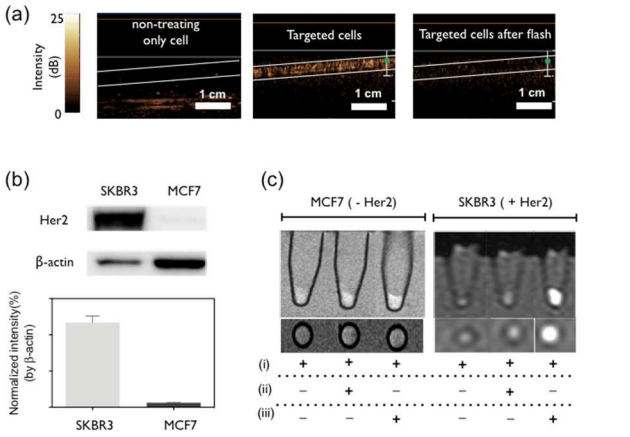

Fig. 3. US and MR imaging of targeted cells, and the effect of flash stimulation; In a phantom US study (iU22, Philips), the treated SKBR3 cell solution revealed significantly high echogenicity as compared to the non-treated cell solution (a, left and middle, MI = 0.08). The signal completely disappeared after 6 flashes (a, right, Fig. S4b). The HER2 positive SKBR3 and negative MCF7 cells were characterized for the expression levels of HER2 receptor with western blotting (b). Following a US flash, the treated cells exhibited a remarkable T_1-*w* MR contrast signal for SKBR3 as compared to the control cells (c, i: flash, ii: MNP(Fe)-HER2, iii: ML-MNP(Fe)-HER2).

To investigate the specific targeting ability and uptake enhancement by US stimulation, the prepared particles were incubated with breast cancer cells. The fluorescent dyes and MNPs were analyzed using CLSM and bio-TEM (Fig. 2). The HER2 expressed positive cells (SKBR3) were treated with a M_GL_R-MNP(Fe)-HER2 particle solution (1 mL, 0.33 mg/mL PBS buffer) for 1 h at 37 °C inside a 5 % CO_2 incubator. During the treatment, the particles adhered just to the cell membrane and not penetrated into the cytoplasm due to the large-sized

MBs. However, the M_GL_R-MNP(Fe)-HER2 particles could be exploited to significantly improve the delivery of Lipo and MNP(Fe) particles into cells; burst of MBs at the flash mode not only released the attached Lipo and MNP(Fe) particles, but also enhanced the permeability of the cell membrane (sonoporation) for more efficient particle uptake.[22] We first investigated such effects *in vitro*. As a result, the HER2 positive cells exhibited green and red fluorescence in the cytosol, and their intensity was analyzed using flow cytometry (ESI Fig. S3**)**. In comparison, HER2 negative cells (MCF7), which underwent the same treatment with the M_GL_R-MNP(Fe)-HER2 particles, demonstrated small amounts of particle inclusion in the cytosol that might be progressed by macropinocytosis, mostly of which were due to non-specific uptake.[23] The particle system thus showed selective delivery to specific cancer cells and the uptake efficiency improved significantly with the external US flash. To realize the uptake mechanism during flash (ESI Fig. S4), the targeting effect was rarely observed after pre-treating with 0.1 % sodium azide at 4 ºC or hyperosmotic 0.45 M sucrose, which inhibit cell metabolism, and the particles were located on the outer cell membrane when incubated at low temperature (4 ºC). From these data, we suggested the involvement of a clathrin-mediated and energy-dependent endocytosis mechanism.

Cell viability after targeting and flash treatment was determined using a typical cell proliferation assay (3-(4,5-Dimethylthiazol-2-yl)-2,5-Diphenyltetrazolium bromide, MTT), where we measured the effects of particle concentration and incubation time. The cells demonstrated a survival rate > 90 % (Fig. 2c). We further investigated the biocompatibility of the particles through an assessment of cellular organelle functions [e.g., the voltage-dependent anion channel, (VDAC; mitochondria function-related protein), Nucleoporin p62 (a protein complex associated with the nuclear envelope), and the anti-apoptotic protein BAD (Bcl-2-associated death promoter)] (Fig. 2d). All markers elicited similar expression levels in the treated and the non-treated control cells, and the US flash stimulation did not cause any cytotoxicity or functional abnormality.

Next, we compared the imaging modality of the prepared M_GL_R-MNP(Fe)-HER2 particles with a commercial clinical US (SonoVue®, Bracco) or T_1-*w* MR (Gadovist®, Bayer Schering Pharma) agents. As a US image contrast agent, the prepared particles displayed similar echogenicity with SonoVue®, as determined by a clinical US scanner (iU22, Philips, Bothell, WA, USA, Fig. S4). Furthermore, the particles showed a 2-fold higher T_1-*w* MR contrast signal than the Gadovist®, as seen on a 0.47 T magnetic relaxometer (r_1 = 6.7 $mM^{-1}{\cdot}s^{-1}$, mq-20, Bruker). A comparative study of the MR phantoms confirmed the superiority of the particles as T_1-*w* MR contrasts agent, as they elicited the same signal strengths at approximately 2-fold lower doses (Fig. S6).

To realize specific cancer cell US imaging capability, SKBR3 cells were targeted with the particles and then harvested in PBS buffer (see ESI). The solution was then transferred to a 5-mm plastic-tube, and showed a significant US echogenicity under the normal imaging-mode illumination (MI = 0.08) due to the intact MBs attached onto the cell membrane (Fig. 3a). After applying US flash (MI = 0.61), the MB was completely destroyed (cavitated), thereby reducing the echogenicity within 6 flashes (ESI Fig. S5b).

To monitor the US flash-mediated enhancement of T_1-*w* MR imaging, the HER2 positive (SKBR3) and negative (MCF7) cells underwent particle targeting (Fig. 3b**)**, flash exposure (1 min), and residue removal. The treated cells were used for MR imaging (3.0-T, Philips, Fig. 3c). The flash-treated cells (in the absence of particle treatment) showed the lowest T_1-*w* MR signal regardless of their HER2 expression. The MNP(Fe)-HER2 (without the ML complex) elicited a low signal as well, indicating that the antibody-conjugated MNP(Fe) particles were not sufficient to increase the MR imaging efficiency by themselves. However, the M_GL_R-MNP(Fe)-HER2- and flash-treated SKBR3 cells revealed a remarkably high contrast image that might be increased internalization of particles owing to the sonoporation effect. Finally, we determined the efficiency of the complex particles for gene delivery. The gene for Survivin (*siSurv*) is a well-known therapeutic gene, which triggers cell apoptosis; the siRNA for Survivin (*siSurv*, 19-mer, Thermo-scientific) can be incorporated inside the Lipo particles.[24] Briefly, the lipid film was lyophilized and homogenized with a complex solution of *siSurv* (50 μM) and a protamine (PA, 7.5 kDa, 40 μM), at a ratio that was optimized to 1.25 genes per PA, using the electrophoretic protocol (Fig. 4a**,** see the experimental section) and characterized the charge change by zeta-potential study (ESI Fig S7). The loading capacity was ≈ 82 %, as determined by UV-Vis spectroscopy (Fig. 4b). The *siSurv*-PA incorporated Lipos were attached to the MB (ML_{siSurv}) and then anchored and conjugated to MNP(Fe) and the HER2 antibody, as described previously. This gene incorporation did not alter the particle system, as evident from the comparison of the morphology and particle size, with ML-MNP(Fe)-HER2 serving as a reference. The

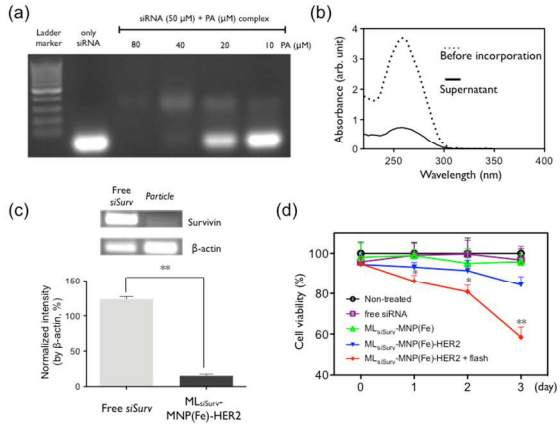

Fig. 4. Therapeutic applications of siRNA *in vitro*; To incorporate the therapeutic gene, the siRNA for Survivin was blended with protamine (PA) through an electrostatic interaction between the two. The optimal complex ratio (50 μM *siSurv* and 40 μM PA) was determined using electrophoresis (a). The loading efficiency of the *siSurv*-PA complex in the Lipo was calculated by monitoring the absorption spectra generated by UV-Vis spectroscopy (b). The target protein showed 8-fold reduced expression levels, relative to the cells with *siSurv* only, as evident from western blotting (c). After treatment, cell viability was monitored as a function of time. The ML_{siSurv}-MNP(Fe)-HER2 and flash treated cells showed a significant decrease in viability (< 60 % viable) in 3 days, while the other controls showed maintained ~ 90 % viability (d). (All experiments in c and d were performed in triplicate. Data shows mean +/- SD, * $P < 0.05$, ** $P < 0.01$)

target cells (SKBR3) were incubated with the therapeutic particles for 1 h, and were then subjected to US flash (1 min). The carrier gene was effectively internalized into the cell owing to the US-mediated uptake enhancement process such uptake effectively down-regulated Survivin expression in these cells as compared to the controls (Fig. 4c). The cell viability following the siRNA delivery decreased to < 60 % after 72 h of the flash, but the control cells exhibited a cell survival rate of > 90

% (Fig. 4d). These results showed that the MB-based particle system was able to enhance the selective transfection efficiency of the bio-molecules incorporated into the linked Lipo.

In summary, we have prepared a hybrid multifunctional particle comprising of MB, Lipo, and MNP(Fe). The resulting complex particles showed high biocompatibility and selectivity, demonstrating multi-modal imaging capability for fluorescence, US, and MR. Interestingly, the linked therapeutic Lipos and MNP(Fe)s rapidly penetrated into the cancer cells after being exposed to US flash, and eventually enhanced the therapeutic effects and MR imaging due to MB cavitation and sonoporation. As a non-toxic theranostic material, the hybrid complex could be readily extended to US and MR-guided cancer treatments in clinical applications.

The authors thank J. B. Park, S. H. Jung, and Y. H. Song for their help in performing the US and MRI measurements and Dr. H. Shao for reviewing the manuscript. This work was supported by a grant from the National Research Foundation of Korea (the Basic Science Research Program 2010-0008846 to T. J. Yoon and 2010-0009271 to H. J. Lee) and partially funded by a grant from the O-song Medical Innovation Foundation R&D project (HO13C0009) of the Ministry of Health and Welfare in South Korea. K.N. Yu was partially supported by a National Research Foundation Grant (NRF-2013-H1A2A1034803) funded by the Ministry of Science, ICT & Future Planning. This study was partially supported by the National Research Foundation of Korea (NRF) funded by the Ministry of Science, ICT & Future Planning (NRF-2012M3A9B4028569)

Notes and references

[a] Department of Radiology, Seoul National University College of Medicine and Seoul National University Bundang Hospital, Seungnam 463-707, South Korea
Program in Nano Science and Technology, Department of Transdisciplinary Studies, Seoul National University Graduate School of Convergence Science and Technology, Suwon 443-270, South Korea
Nanoimaging and Therapy Research Center, Institute of Nanoconvergence, Advanced Institutes of Convergence Technology, Seoul National University, Suwon 443-270, South Korea
[b] Materials Chemistry Laboratory, Department of Chemistry, Seoul National University, Seoul 151-742, South Korea
[c] Address here. Bio-Nanomaterials Chemistry Laboratory, Department of Applied Bioscience, College of Life Science, CHA University, Pocheon 135-081, South Korea
Nanoimaging and Therapy Research Center, Institute of Nanoconvergence, Advanced Institutes of Convergence Technology, Seoul National University, Suwon 443-270, South Korea
E-mail: tjyoon@cha.ac.kr
[d] Laboratory of Toxicology, College of Veterinary Medicine, Seoul National University, Seoul 151-742, South Korea
[e] Laboratory animal center, KBIO Osong Medical Innovation Foundation, Osong, Cheongwon, Chungbuk 363-951, South Korea
[f] Department of Biomedical Science, College of Life Science, CHA University, Pocheon 135-081, South Korea
[g] They contributed equally to this work.

Electronic Supplementary Information (ESI) available: Synthetic procedures and characterization data for ML-MNP (Fe)-HER2 hybrid particles. Details pertaining to other evidences, results, data, and experimental methods are included. See DOI: 10.1039/c000000x/

1 X. Xie, S. Lee and X. Chen, *Adv. Drug Deliv. Rev*. 2010, **62**, 1064-1079.
2 H. L. Liu, C. H. Fan, C. Y. Ting and C. K. Yeh, *Theranostics,* 2014, **1**, 432-444.
3 P. Prabhu and V. Patravale, *J. Biomed. Nanotechnol.*, 2012, **8**, 859-882.
4 W. Wu, Q. Zhang, J. Wang, M. Chen, S. Li, Z. Lin and J. Li, *Polym. Chem.,* 2014, **5**, 5668-5679.
5 W. Wu, J. Wang, Z. Lin, X. Li and J. Li, *Macromol. Rapid Commun.,* 2014, **35**, 1679-1684.
6 Z. Zhou, L. Wang, X. Chi, J. Bao, L. Yang, W. Zhao, Z. Chen, X. Wang, X. Chen and J. Gao, *ACS Nano,* 2013, **7**, 3287-3296.
7 H. Yoo, S. K. Moon, T. Hwang, Y. S. Kim, J. H. Kim, S. W. Choi and J. H. Kim, *Langmuir,* 2013, **29**, 5962-5967.
8 A. Gojova, B. Guo, R. S. Kota, J. C. Rutledge, I. M. Kennedy and A. I. Barakat, *Environ, Health Perspect.*, 2007, **115**, 403-409.
9 S. T. Yang, J. H. Liu, J. Wang, Y. Yuan, A. Cao, H. Wang, Y. Liu and Y. Zhao, *J. Nanosci. Nanotechnol.*, 2010, **10**, 8638-8645.
10 R. Yoke, E. Grulke and R. MacPhail, *Wiley Interdiscip. Rev. Nanomed. Nanobiotechnol.*, 2013, **5**, 346-373.
11 S. Capece, E. Chiessi, R. Cavalli, P. Giustetto, D. Grishenkov and G. Paradossi, *Chem. Commun.*, 2013, **49**, 5763-5765.
12 F. Y. Yang, T. T. Wong, M. C. Teng, R. S. Liu, M. Lu, H. F. Liang and M. C. Wei, *J. Control Release*, 2012, **160**, 652-658.
13 Y. I. Yoon, Y. S. Kwon, H. S. Cho, S. H. Heo, K. S. Park, S. G. Park, S. H. Lee, S. I. Hwang, Y. I. Kim, H. J. Jae, G. J. Ahn, Y. S. Cho, H. Lee, H. J. Lee and T. J. Yoon, *Theranostics*, 2014, **4**, 1133-1144;
14 A. T. Nguyen and S. P. Wrenn, *Wiley Interdiscip. Rev. Nanomed. Nanobiotechnol.*, 2014, **6**, 316-325.
15 F. Yang, Y. Li, Z. Chen, Y. Zhang, J. Wu and N. Gu, *Biomaterials*, 2009, **30**, 3882-3890.
16 K. Y. Ju, J. W. Lee, G. H. Im, S. Lee, J. Pyo, S. B. Park, J. H. Lee and J. K. Lee, *Biomacromolecules*, 2013, **14**, 3491-3497.
17 P. Prentice, A. Cuschieri, K. Dholakia, M. Prausnitz and P. Campbell, *Nat. Phys.*, 2005, **1**, 107-110.
18 C. X. Deng, F. Sieling, H. Pan and J. Cui, *Ultrasound Med. Biol.*, 2004, **30**, 519-526.
19 H. Lee, S. M. Dellatore, W. M. Miller and P. B. Messersmith, *Science*, 2007, **318**, 426-430.
20 C. Owen, N. Patel, J. Logie, G. Pan, H. Persson, J. Moffat, S. S. Sidhu and M. S. Shoichet, *J. Control. Release*, 2013, **172**, 395-404.
21 A. S. Manjappa, K. R. Chaudhari, M. P. Venkataraju, P. Dantuluri, B. Nanda, C. Sidda, K. K. Sawant and R. S. Murthy, *J. Control. Release*, 2011, **150**, 2-22.
22. Y. Hu, J. M. Wan, A. C. Yu, *Ultrasound Med. Biol.* 2013, **39**, 2393-2405.
23 B. D. Meijering, L. J. Juffermans, A. Wamel, R. H. Henning, I. S. Zuhorn, M. Emmer, A. M. Versteilen, W. J. Paulus, W. H. Gilst, K. Kooiman, N. Jong, R. J. Musters, L. E. Deelman and O. Kamp, *Circ. Res.,* 2009, **104**, 679-687.
24 M. A. Arangoa, N. Duzgunes and C. Tros de llarduya, *Gene Ther.* 2003, **10**, 5-14.